The Controlling Chemistry of Surface Deposition from Sodium and Potassium Seeded Flames Free of Sulfur or Chlorine Impurities

MARTIN STEINBERG and KEITH SCHOFIELD*
Materials Research Laboratory, University of California, Santa Barbara, CA 93106, USA

Sodium and potassium salt deposition have been studied in a series of propane and hydrogen flames free of sulfur or halogen impurities. With the collection probe in the 400 to 800 K range, samples of pure carbonate are observed and more importantly the rates of, for example, sodium carbonate deposition measured in terms of alkali metal are identical to those previously reported for sodium sulfate formation and also those observed for dominant NaCl deposition. Moreover, the behavior of Na_2CO_3 deposition mirrors exactly that of Na_2SO_4 in this temperature range. It shows a corresponding first order dependence on flame total sodium concentration, a zero order dependence on flame carbon, an insensitivity to fuel type, equivalence ratio, flame temperature, flow rate, probe material, or the nature of the sodium speciation in the flame, be it atomic or the hydroxide, or the state of the flame equilibration. A constant rate of deposition between 330 and 800 K conveys formation kinetics with a zero activation energy and that the surface accommodates atomic sodium equally well, be it below or above its dew point temperature and also at a seemingly approximately equal rate to that of flame NaOH. The fact that Na_2CO_3 cannot exist in the gaseous state in a flame finally proves irrefutably that these alkali deposition processes producing sulfate, carbonate or halide salts are heterogeneous in nature. The high collection efficiencies of the surface for alkalis have been confirmed by a further independent new calibration method for flame total alkali content. Also deposition rates are seen to be extremely similar in C_3H_8/O_2 flames heavily diluted with either He, Ne, or Ar and also in a very fuel rich H_2 or D_2 flame. As with sulfate deposition, the rate of deposition is predominantly controlled by the actual flux of alkali in the flame gases that are intercepted by the collection probe. Moreover, there is an insensitivity to probe geometry and the nature of the flame flowfield, be it laminar or turbulent. The theoretical understanding of the complex boundary layer penetration and deposition mechanism is still inadequate in explaining these observations. The most intriguing results and differences from sulfate deposition have been observed on probes at lower temperatures (330–370 K). Although the formation of $NaHCO_3$, and more so $KHCO_3$, was expected to compete with that of their carbonates, in the case of sodium under fuel lean conditions only a small competing contribution of $NaNO_3$ formation was noted. This was very marginal for fuel rich conditions. However, with potassium the effects were enhanced and KNO_3 competes significantly with K_2CO_3 under fuel lean conditions. However, in fuel rich flames an unexpected dominant formation of potassium oxalate, $K_2C_2O_4$, was observed, along with some K_2CO_3 and a small amount of $KHCO_3$. Thermodynamic expectations in this lower temperature regime tend to suggest nitrate>bicarbonate>carbonate>oxalate. This is our first clearly observed non-equilibrium deposition behavior where the flame begins to display a pivotal role in controlling the surface molecular distribution. It also raises the possibility that low temperature surfaces in flames may be a new route for synthesizing certain thermodynamically metastable materials.

INTRODUCTION

This is the second [1] in a planned series of papers that relate to the chemical characterization of alkali salt deposition in combustion systems. For a long time, there has been a need to understand in quantitative terms the controlling aspects of high temperature corrosion which is known to result primarily from alkali sulfates and chlorides [2–4]. Such salts, particularly when molten, act as a flux on the surface, removing protective oxide layers. They invariably can lower the melting points of other materials and generally lead to severe corrosion. Previously, most studies have been concerned mainly with Na_2SO_4 formation. In this regard, a very significant effort was made over the years by the group at NASA Lewis Research Laboratory and was published in an extensive series of NASA reports and journal articles, but a clear understanding of the processes involved was never realized [5–11]. Nor was the question answered as to whether the formation of Na_2SO_4 was homogeneous in the flame environment or heterogeneous on ash particles or intercepted surfaces. In recent years, particu-

*Corresponding author. E-mail: combust@mrl.ucsb.edu

COMBUSTION AND FLAME 129:453–470 (2002)

Published by Elsevier Science Inc.
0010-2180/02/$–see front matter
PII S0010-2180(02)00363-2

larly with newly proposed policies to emphasize the use of biomass as an energy fuel [12–16], and with certain problems in fluidized bed combustion [17, 18], a significant renewed interest has re-emphasized the importance of understanding high temperature corrosion and related deposition processes. At present, the problem is in fact a restriction to the technological development of gas turbines and is a major reason for their predominant use of natural gas fuel [19].

Our earlier work on homogeneous interactions of sodium and sulfur in the burned gases of flames implied that kinetic limitations ruled out a flame homogeneous Na_2SO_4 formation mechanism [20, 21]. The initial work on Na_2SO_4 deposition [1] established that formation was indeed a surface phenomenon and occurred at a rate that was directly proportional to the flame total sodium content. It was independent of the chemical nature of the sodium in the burned gases and the surface processed all the flame sodium forms, atomic, NaOH and even NaCl as being equivalent. Moreover, rates of Na_2SO_4 formation were seen to be independent of fuel type, equivalence ratio, flame temperature and not affected by the state of non-equilibrium in the fuel rich or lean flames studied. The surface domain appeared to be all-controlling, using the flame solely as a source of any required ingredients. As long as there was sufficient sulfur in the flame to satisfy the formulation Na_2SO_4, or in other words $[S] \geq 0.5[Na]$, Na_2SO_4 formation was seen to be dominant and displayed a zero order dependence on the sulfur flame concentration. This finding clearly dashed the hopes that reduced corrosion might result from lowering fuel sulfur levels. It also raised the intriguing question as to the nature of the behavior when sulfur levels are reduced below those of the alkali and when sulfur is not present at all. This latter aspect forms the basis of the present paper.

In practical terms, fuels that contain sodium invariably contain sulfur and chlorine. As a result, the deposition of sodium from relatively 'clean' flames has hardly been examined. Dunderdale and Durie's study [22], 37 years ago, was an important first attempt to systematically examine the nature of sodium flame deposits. By X-ray analysis, they noted when sodium or calcium salts were present in stoichiometric propane/air flames that deposition collection probes at 723 K indicated the formation of Na_2CO_3 or $CaCO_3$, respectively. More recently, K_2CO_3 deposits have been reported on electrodes in MHD experiments using a potassium seeded, LPG/O_2 combustor plasma [23]. Although not directly related to corrosion problems, as will be seen, this possibility of inducing alkali carbonate or other salt deposition has resulted in significant additional insights into the general behavior of sodium deposition.

In the first place, alkali carbonates or bicarbonates are not particularly stable in the gas-phase. They certainly cannot exist homogeneously in the burnt gases of flames. Hildenbrand and Lau [24] endeavored to monitor gaseous $NaHCO_3$ in experiments at about 1100 K in equilibrated Knudsen cell, mass spectrometric experiments but were unsuccessful. Their measurements did provide an upper bound on the stability of $NaHCO_3$(g). This was compatible with mesospheric models of sodium chemistry which are at much lower temperatures. In the upper atmosphere, $NaHCO_3$(g) currently is regarded as the major sink for sodium to lower altitudes [25–28]. Although Na_2CO_3(s) is very stable, it vaporizes predominantly by dissociation. In equilibrated vaporization studies of Na_2CO_3(s) in a Knudsen cell at its 1123 K melting point, the fraction of vapor that is Na_2CO_3(g) is only about 0.01% [24]. As a result, carbonate deposition is necessarily a heterogeneous process. Moreover, carbonate deposition provides an alternate and very complementary system against which sulfate or halide deposition behavior can be compared. Although the deposition of sodium has been emphasized in this program, some corresponding measurements also are reported for potassium.

EXPERIMENTAL

The burner and flow system have been described previously [1]. The 1-D flat flames are premixed, have laminar vertical flows and are at atmospheric pressure. Flames studied include C_3H_8/air with equivalence ratios of 0.8 to 1.2 and some with reduced N_2 content to elevate

their temperatures. $H_2/O_2/N_2$ flames had fuel lean to rich ratios of 1.4/1/5, 1.8/1/3, 2.2/1/6, and 4/1/6. These generally utilized compressed air as their source of O_2 and so contained a slight natural CO_2 content. Occasionally, ultra-high purity $H_2/O_2/N_2$ flames were burned to more carefully control the flame carbon content. Flames of $C_3H_8/O_2/Rg$ were compared with Rg = He, Ne, or Ar and on one occasion fuel rich $H_2/O_2/N_2$ and $D_2/O_2/N_2$ (6/1/5) were used. Flame temperatures generally have been in the range 1700 to 2650 K. The faster burning H_2 flames provide for better spatial and hence time resolution and were used primarily for an examination of possible flame non-equilibrium effects, and for examining flames of low carbon content.

Flame concentrations of sodium in the 5 to 60 ppm range have been found adequate to produce measurable probe deposits in an acceptable period of time (1–6 h). Sodium was introduced into the premixed unburned gases as an aqueous aerosol from an ultrasonic nebulizer. Solution strengths up to 0.1 N with respect to sodium have been used. The solutions contained a trace of potassium (K:Na = 0.5%) to facilitate monitoring the optically thin potassium resonance line emission as a measure of constancy of aerosol delivery into the flame. The burner and delivery line were heated to minimize aerosol loss. Generally, this permitted operation for periods of up to 8 to 10 h of constant conditions before the flow lines and burner had to be cleaned and re-dried. For this program, various sodium salt solutions were used, namely the nitrate, nitrite, formate, oxalate, glycinate, and bicarbonate. These were all equivalent sources of sodium being fully dissociated in the flame's reaction zone.

The deposit collection probes were cylindrical and generally about 12 mm in diameter. The probe essentially intercepts all of the seeded inner core burner flow at some point. Probes were constructed of Inconel-600 stainless steel and had a central channel down their length for air or water cooling. They also had a thermocouple within the wall to accurately monitor probe surface temperatures. One probe was tightly clad with a 0.05 mm thick foil of platinum. This was used occasionally to ensure clean deposits that were not contaminated with probe corrodants. The probe was mounted horizontally in the vertical burned gas flow and the burner platform raised or lowered by a computerized stepper motor. In this way, the flame could be studied as a function of downstream times. In this paper, results are presented for probe temperatures in the 330 to 975 K range.

Deposits have been characterized mainly by Fourier Transform Raman spectroscopy which is ideally suited to alkali salt analysis. A Nicolet spectrometer has been used with a 1.06 μm Nd.YAG laser excitation source. Occasionally, an alternate home built system based on the shorter wavelength Ar^+ laser line excitation has been used to identify interfering crystal luminescences and confirm the true Raman spectral features. After a sample has been collected on the probe in the flame it is cooled in a flow of prepurified nitrogen. The powdery sample is easily removed from the probe and instantly transferred into a 1.5 mm diameter glass capillary tube and sealed. In this way contact with air is very minimal. Samples of 5 to 10 mg are quite sufficient for spectral analysis. During the course of an experiment it is also common for a deposit to appear as a honeycomb shape on top of the multi-holed burner. These burner top samples were more prevalent with the slower burning propane flames but could occasionally build up with time, even with the faster flow hydrogen flames. These samples also were removed and analyzed. Rates of deposition were measured by dissolving the sample off the probe with a known volume of de-ionized water and analyzing for total sodium. Either a Thermo Jarrell Ash High Resolution ICP or a flame photometric Beckman analytical burner were used for this purpose. Comparisons between the two methods indicated very close agreement.

In several instances additional information concerning deposit structure and purity was obtained by X-ray powder crystallography and by Na/H/C/N chemical analysis.

RESULTS AND DISCUSSION

Flames of propane or hydrogen (containing traces of CO_2 in the air supply), with low levels of sodium, produced smooth white deposits on a probe with little difficulty. An examination of

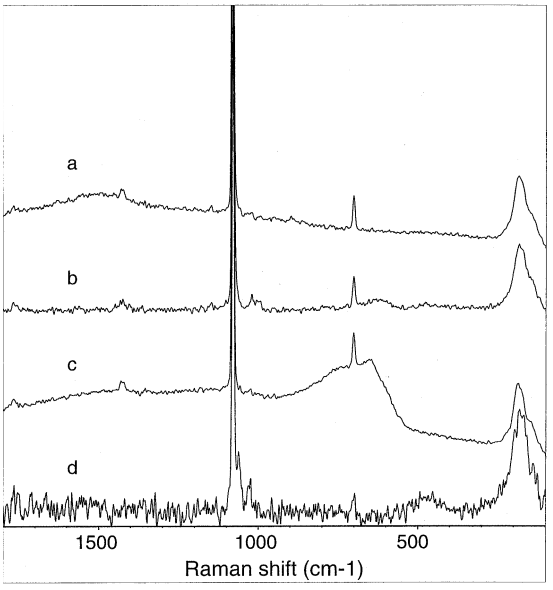

Fig. 1. Raman spectra of deposits collected on a probe in a variety of flames. (a) $\phi = 0.8$ C_3H_8/air, stainless steel probe at 682 K, 8 ms downstream, 60 ppm sodium flame density. (b) $\phi = 1.2$ C_3H_8/air, platinum clad probe at 725 K, 3.7 ms downstream, 40 ppm flame sodium. (c) Ultrahigh purity $D_2/O_2/N_2$(1.4/1/5), platinum clad probe at 725 K, 3 ms downstream, 25 ppm flame sodium and Na: C = 1:1. (d) $H_2/O_2/N_2$(air), (2.2/1/6), stainless steel probe at 725 K, 4 ms downstream, 9 ppm flame sodium and 190 ppm flame CO_2. All flames used $NaNO_3$ aqueous aerosol additive except (c) which used sodium oxalate. The slight splitting in (d) results from some sample absorption and crystallization of water to produce a small amount of $Na_2CO_3.H_2O$.

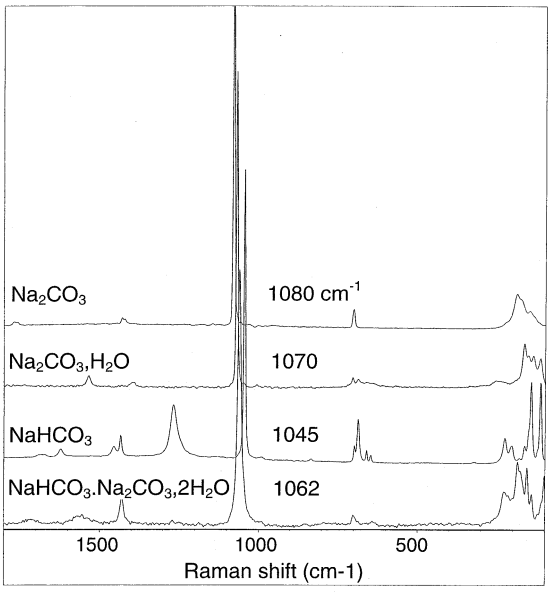

Fig. 2. Raman reference spectra of pure samples of Na_2CO_3, $Na_2CO_3.H_2O$, $NaHCO_3$ and the sesquicarbonate salt $NaHCO_3.Na_2CO_3.2H_2O$.

their Raman spectra is illustrated for various cases in Fig. 1. For comparison, spectra of pure, purchased samples of Na_2CO_3, $Na_2CO_3.H_2O$, $NaHCO_3$, and the sesquicarbonate, $NaHCO_3.Na_2CO_3.2H_2O$ are illustrated in Fig. 2. The structural presence of the H-atom in the bicarbonate modifies its Raman spectrum from that of the carbonate. As seen at higher resolution, and even in Fig. 2, it perturbs the Raman shift or vibrational frequency of the predominant carbonate anion from 1080 cm^{-1} for the carbonate to 1045 cm^{-1} for the bicarbonate, and introduces other spectral frequencies that are easily detected experimentally. In this work, spectra generally were recorded with a spectral resolution of 4 cm^{-1}. It became clear almost immediately that essentially pure Na_2CO_3 is deposited in all cases where the probe has an elevated temperature. Occasionally, the very hygroscopic pristine carbonate deposit did manage to absorb a little air moisture in the brief handling procedure, apparent in the Raman spectra, by a smaller peak shifted 10 cm^{-1} to 1070 cm^{-1}. Further water absorption should make no change as the spectrum of $Na_2CO_3.10H_2O$ is identical to that of $Na_2CO_3.H_2O$.

This carbonate formation, illustrated in the four cases of Fig. 1, is independent of fuel type, equivalence ratio, flame temperature or probe material. As will be discussed in more detail later, only at very low probe temperatures do changes begin to be seen and carbonate loses some of this dominance. Additional analyses using X-ray powder crystallography and Na/C/H/N chemical composition analyses confirmed that, except at low temperatures (300–400 K), the carbonate was the sole predominant product and that the sample did not contain any other Raman inactive materials such as NaOH. This has been further validated in work on Na_2SO_4 /Na_2CO_3 deposited mixtures that will be published in a subsequent paper. In such cases a 100% mass balance for deposited sodium has been derived for the two salts, confirmed by a combination of ICP and Raman measurements.

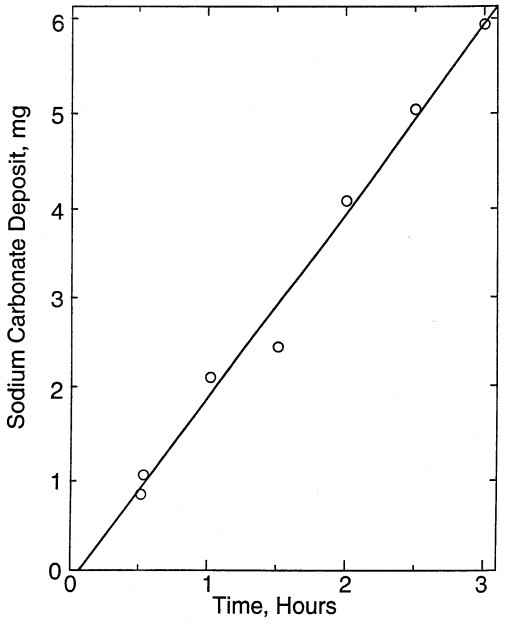

Fig. 3. Quantity of Na_2CO_3 deposited as a function of time on a stainless steel probe at 750 K located 5 ms downstream. $\phi = 0.9$ C_3H_8/air flame, 30 ppm flame sodium from $NaNO_3$ aqueous aerosol.

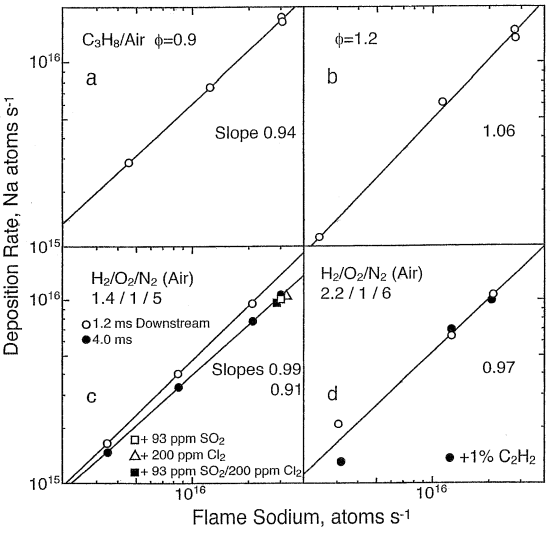

Fig. 4. First-order dependences of the rates of deposition of Na_2CO_3 on flame sodium concentration (from $NaNO_3$) in a series of propane and hydrogen flames. Collected on a stainless steel probe at about 720 K, $\phi = 0.9$ (7.4 ms downstream), $\phi = 1.2$ (4.4 ms) and 2.2/1/6 (4.0 ms).

Rates of Deposition and Sodium Dependence

As indicated in Fig. 3, for a specific set of conditions, the formation of the Na_2CO_3 deposit shows a linear growth rate. Moreover, on all the deposition probes used, new or old, platinum or stainless steel, there appears to be no measurable incubation period. In this case, the rates of deposit that were measured approximated to 2 mg Na_2CO_3/h. Taking an average density for the deposit, this implies very approximately that about two molecular layers are deposited per second. Because the exact density of the sample remains uncertain, this is a very rough estimate. Nevertheless, it illustrates to some degree what is happening on the surface at the molecular level. Consequently, within a very short time period the deposit is growing on its own crystal latticework. Whether the underlying metal substrate retains any influence remains an interesting question but we observe no probe material dependences.

By varying the solution strength in the nebulizer it was possible to quantitatively vary the sodium in the flame. In this way, rates of deposition of Na_2CO_3 could be accurately measured as a function of total flame sodium content. As illustrated in Fig. 4, a pronounced first order dependence is evident and rates of deposit are directly proportional to the quantity of sodium addition. This has been found to hold true for any of the flames and the range of probe temperatures reported in this paper. The observed correlation displays unit slopes within experimental error. The hydrogen flames contained ambient air from a compressor that introduced about 230 and 190 ppm CO_2, respectively, to the 1.4/1/5 and 2.2/1/6 ($H_2/O_2/N_2$) flames. As seen in Fig. 4d, addition of extra carbon in the form of a 1% C_2H_2 addition to the 2.2/1/6 flame made an insignificant difference.

Figure 4c shows rates of deposition at two downstream flame locations, 1.2 and 4.0 ms from the reaction zone of a fuel lean hydrogen flame. This is a non-equilibrated flame and our previous measurements have indicated that H, OH and O atom radical densities decay by factors of about 45, 3.6, and 15-fold, respectively, between the two locations. Also, flame sodium speciation also changes by an order of magnitude, being close to 90% atomic sodium at 1.2 ms and about 90% NaOH at 4.0 ms [29]. However, despite these drastic variations in flame composition, the deposition behavior is

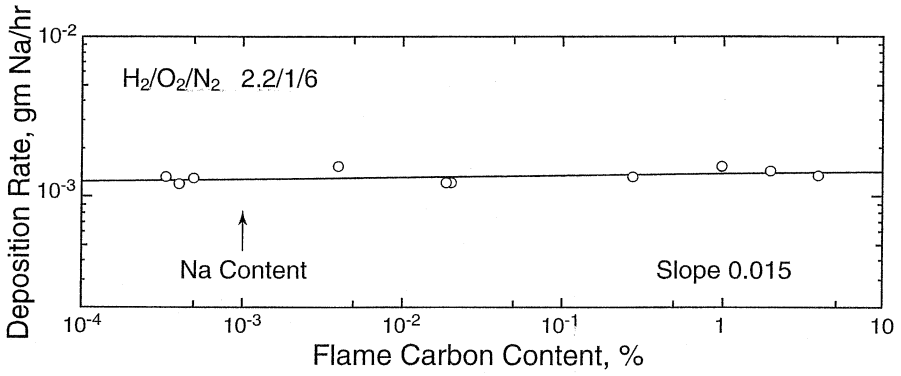

Fig. 5. Zero-order dependence of the rates of deposition of Na_2CO_3 on flame carbon content (measured as % by volume in the unburned gases). Flames of H_2/air/N_2 some with added C_2H_2, or ultra-high purity $H_2/O_2/N_2$ gases were used, additionally with boiled nebulizer solutions for the ultra-low values. Stainless steel and platinum clad probes were located 4 ms downstream and maintained at 720 K. Sodium flame content approximated to 10 ppm (1×10^{-3}%).

very similar at the two locations. Similar results were seen previously for Na_2SO_4 deposition [1]. As in that case, the observed slight variation in the data can be adequately accounted for by the small diffusional lateral spread with time of the sodium concentration in the flame from the inner seeded core flame to the outer protective non-seeded shield flame. This reduces the intercepted sodium flame density slightly and hence its deposition rate.

Also illustrated in Fig. 4c are some direct comparisons that were made in this flame with the data all being collected on the same day. In this way it is the most reliable and factors out slight day-to-day variations. The rate of deposition of Na_2CO_3 was directly compared to that of Na_2SO_4 formation (when 93 ppm SO_2 was added to the flame), to NaCl deposition (220 ppm Cl_2 flame addition), and to Na_2SO_4 (when 93 ppm SO_2 plus 200 ppm Cl_2 were added). As seen, in all cases the same rates of deposition of sodium are observed within experimental accuracies. The SO_2 experiments fall 4 to 5%, and the Cl_2 addition 6% below that of Na_2CO_3 formation. Accuracies of measurement in this situation are in the ±10%. If there are real differences they are quite small. This is an extremely interesting and unexpected finding with significant implications. It is apparent that the predominant controlling process in the deposition is the rate at which the sodium interacts with the surface. The nature of the flame sodium, be it Na, NaOH, or NaCl, appears irrelevant and the metallic or various salt surfaces onto which the growth is occurring must have extremely similar accommodation coefficients for all of these. Moreover, the data imply that the surface can convert the sodium influx into the respective final composition by processes that are not rate controlling in the overall deposition mechanism.

Insensitivity to Flame Carbon Content

The variation of the rate of deposition of Na_2CO_3 with flame carbon content is illustrated in Fig. 5. It was most extensively studied in a fuel rich $H_2/O_2/N_2$ (2.2/1/6) flame. The quantity of carbon was modified in the 0.24 to 4% range by adding traces of C_2H_2. Values of about 187 ppm CO_2 addition arose by utilizing compressed ambient air as the flame oxygen source. Cleaner carbon-free flames were obtained by turning to ultra-high purity gases and either adding traces of ambient air or by modifying the salt solution in the nebulizer to a sodium nitrate/formate mixture. CO_2 is very soluble in water and the nebulized water added about 3.5 ppm CO_2. This could be reduced by a factor of seven by boiling and then carefully excluding air from the aqueous solution. Irrespective of all the efforts that were taken to carefully modify the flame CO_2 content over a wide dynamic range, the data clearly showed that it was irrelevant. As seen, the deposit rate reflects a zero order dependence on carbon and a regression fit to the data indicated a zero slope to within 1.5%.

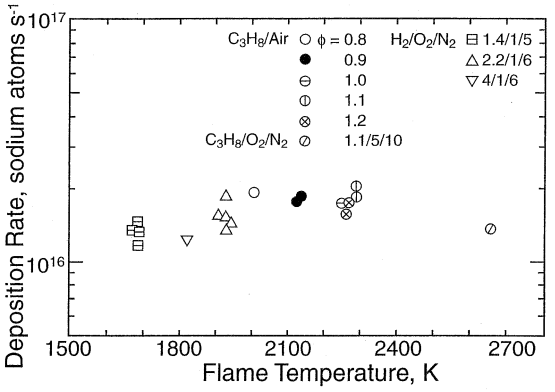

Fig. 6. Rates of deposition of Na_2CO_3 as a function of flame temperature in a wide variety of propane and hydrogen (air supplemented) flames. All refer to a similar sodium flame flux (3.2×10^{16} sodium atoms s^{-1} from $NaNO_3$) and are collected on probes in the range 715 to 770 K located 2.7 to 9.1 ms (C_3H_8 flames) and 1.2 to 4.0 ms (H_2 flames) downstream.

The three points with the lowest flame carbon in Fig. 5 are such that there is less carbon than sodium in the flame. As with Na_2SO_4 formation, there are indications that down to atomic ratios of Na:C = 2:1, Na_2CO_3 remains the dominant sodium product. These lowest points therefore are very marginal in this respect. As the amount of carbon falls to, or below half that of the sodium, indications are that Na_2CO_3 is formed to its full extent, and the remaining sodium becomes NaOH. This was evident in additional experiments at extremely low flame carbon levels in which a known amount of deposit was dissolved in boiled distilled water and its pH value measured. NaOH has a greater alkalinity than Na_2CO_3 and the mix of NaOH/Na_2CO_3 could be calculated. Additionally, as such solutions sat in the ambient air, the pH moderated with time as the NaOH absorbed atmospheric CO_2 and converted to Na_2CO_3.

Dependence of Deposition Rates on Flame Temperature, Equivalence Ratio, or Fuel Type

Figure 6 summarizes the rates of deposition of Na_2CO_3 in a wide variety of flames on collection probes at about 715 to 770 K. All data refer to the same sodium flux intercepting the probe. The observed scatter is not too surprising in that these separate data were measured at various times over a two-year period and refer to a wide variety of flames. They have significantly different burning velocities and the range of flow rates spans a factor of about sevenfold. Nevertheless, it is felt that these data are sufficiently reliable to illustrate an insensitivity to fuel type, equivalence ratio, flame temperature, flow velocities, and probe flame location. It mirrors very similar behavior previously reported with Na_2SO_4 deposition [1]. It again illustrates the paramount dominance of the surface dynamics in the process and the fact that the flame plays only a supporting role. Neither the speciation of the sodium in the flame gases, nor the extent of flame equilibration or its composition appears relevant.

When compared to the flux of total sodium in the flame, the rates of deposition, as with Na_2SO_4, are similarly quite large. They reflect a probe collection efficiency for sodium from the burned gases as previously reported in the 30 to 60% range of the total intercepted sodium flame flux [1]. Since that paper, a newly developed, independent, and alternate calibration method for total sodium flame content has been devised. This will be published separately, but confirms and reaffirms the previous calibrations and collection efficiencies. These deposition processes do not appear to be readily explainable by normally expounded boundary layer diffusion models. Moreover, the process is not unique solely to the alkali species. In experiments in which sulfur is accurately added in the ratio of half that of the sodium, Na_2SO_4 still is dominantly formed, accounting for close to 100% of the sodium. In other words, traces of sulfur must reach the surface with efficiencies equal to those of sodium.

It may be appropriate to illustrate further at this point this current dilemma of flame deposition theory with additional related data. Na_2CO_3 rates of deposition were measured in several propane flames in which the major flame diluent was either He, Ne, or Ar. Being monatomic gases, such flames have very approximately the same temperatures and are similar. In each case a small amount of N_2 passed through the ultrasonic nebulizer to introduce the same flux of aqueous $NaNO_3$ aerosol to the inner flame gas flows. Reduced additions of sodium were used to minimize this N_2 addition. With hindsight, of course, a constant portion of

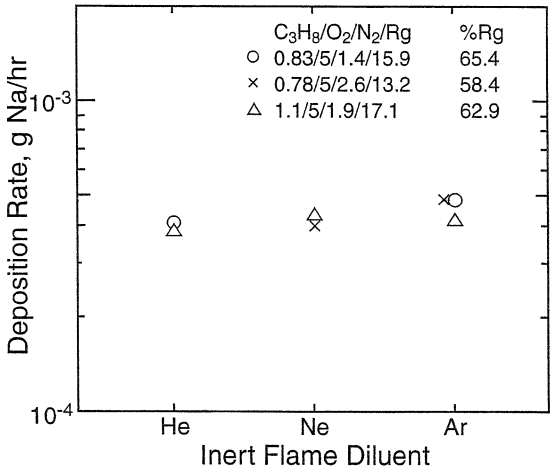

Fig. 7. Rates of deposition of Na_2CO_3 from flames in which the predominant diluent is either He, Ne, or Ar. In all instances the nebulizer operated with a similar low flow of N_2 to maintain a constant delivery of aqueous $NaNO_3$ aerosol. Flames have temperatures in the range 2450 to 2570 K and a sodium content of ~12 ppm. Unburned gas flow rates are the same for $\phi = 0.83$ and 1.1 and the rate halved for $\phi = 0.78$. In each case a stainless steel probe at 750 K is located at either 2.7 ms ($\phi = 0.83$, 1.1) or 5.6 ms ($\phi = 0.78$) downstream. The burned gas content of the inert rare gas is as indicated.

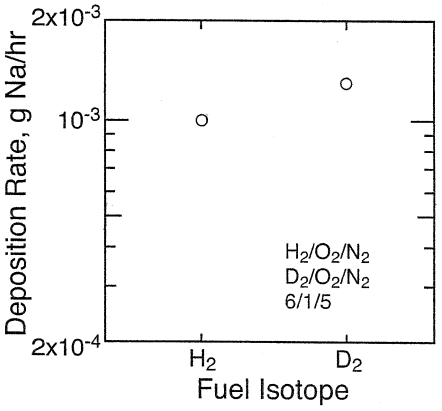

Fig. 8. Measurements of the rates of deposition from a very fuel rich hydrogen or deuterium flame. Flame temperatures are about 1640 K and a solution of sodium formate is used to ensure adequate flame carbon. Sodium flame content is about 20 ppm. A stainless steel probe is located 3.0 ms downstream and maintained at 845 K.

the oxygen flow could equally well have been used to maintain a repeatability of the nebulizer flux and remove this presence of N_2 altogether. Nevertheless, these rather preliminary data, plotted in Fig. 7, are quite sufficient to illustrate the essentially very similar behavior in all three cases. As indicated, the burned gases have compositions that are close to 60% rare gas in each case. For the $\phi = 0.78$ flame diluted with Ne and Ar the flow rate was halved over that used in the other flame cases. The two datum points reflect the common trend and provide assurance of no interfering problems relating to loss in the heated line from the nebulizer or in the burner core. These data were acquired on two consecutive days and should be quite reliable. They also reflect a normal range of scatter for data so collected.

There is a 10-fold difference in mass between He (4.003 atomic weight) and Ar (39.948). Red'ko [30] has indicated that at these temperatures there should be a threefold difference in diffusion coefficients for sodium in helium or argon. As expected diffusion is faster in helium. This certainly is not reflected in Fig. 7. Moreover, in the fuel lean flames the sodium is predominantly NaOH whereas largely atomic in the fuel rich-flame. Again, this apparently is without consequence.

On another occasion, back-to-back measurements were made in very fuel rich H_2 and D_2 flames, burned to maximize their isotopic differences. The burned gases contained about 36.4% H_2 or D_2, and 18.2% H_2O or D_2O. The rates of Na_2CO_3 deposition are shown in Fig. 8. Although there was only sufficient deuterium for one experiment, it is considered reliable and shows a slightly larger rate, again somewhat contrary to mass expectations. Diffusion coefficients for sodium in D_2 or D_2O are expected to be smaller [31].

Also, as will be published in a subsequent paper, deposition rates for all the alkali metals (lithium through cesium) are surprisingly similar despite their 20-fold difference in atomic weights.

Clearly, our understanding remains vague of the processes whereby the sodium manages to penetrate the boundary layer that surrounds the probe and deposit with such high and somewhat constant efficiencies. With concentrations of sodium in the burned gases, that at times can be made quite small, it does appear that the gas-phase has to remain homogeneous well into the boundary layer or even onto the surface. Moreover, any heterogeneous gas-phase mechanisms

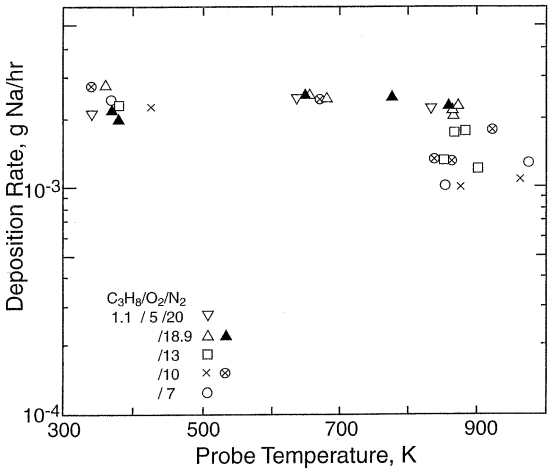

Fig. 9. Rates of deposition of Na_2CO_3 as a function of probe temperature in a number of $\phi = 1.1$, N_2 diluted C_3H_8 flames. The data for each symbol were collected on the same day and are more accurate than a comparison between differing symbols which may have slight day-to-day variations. As N_2 is decreased the five compositions have approximate flame temperatures and probe locations of 2200 K (5.1 ms), 2285 (3.2), 2520 (3.0), 2650 (2.9), and 2780 (1.8), respectively.

would undoubtedly introduce gas-phase dependences and result in variations that are not evident. The fluid dynamical analysis of such systems is highly complex and has to necessarily invoke certain assumptions or models. It does appear that the previous attempts [7, 11], still the current state of the art, are inadequate and require a detailed re-examination.

Deposition Rates as a Function of Probe Temperature

Cooling the probe by passing air or water through its inner core, and by using flames of differing temperatures (enthalpies), it has been possible to measure the rates of deposition on probes as a function of temperature. These data are indicated in Fig. 9. In the range 340 to about 800 K very similar rates are obtained for carbonate deposition with little variance. It might be added that this reflects and is identical to that also seen in sulfate or chloride deposition experiments. This constancy is quite remarkable and implies not only that the chemistry is similar through this regime but also that the surface kinetic processes must be very rapid. It reflects a zero activation energy for the chemistry down to at least 340 K. The chemistry, per se, is not rate controlling as evidenced by the lack of sensitivity as to whether carbonate or sulfate is formed. It is the influx of alkali that is governing the overall process. This same behavior is seen whether flames are fuel-rich or lean. This is additionally interesting in that the ratio of gaseous Na to NaOH in such flames varies over a considerable range and further implies a very similar surface accommodation coefficient for the two. The melting point of sodium is 371 K and at 800 K its vapor pressure is about 9×10^{-3} atm (6.9 torr). As a result, the dew point of gaseous atomic sodium at a flame concentration of about 30 ppm is close to 580 K. On the other hand, NaOH has a melting point of 591 K, is very stable in its gaseous form, and has a boiling point of 1663 K. Its vapor pressure is much smaller and at 800 K is of the order 10^{-7} atm. Consequently, in this present probe temperature range, atomic sodium will be both above and below its dew point with respect to the surface, whereas NaOH will always favor condensation. Although the probe surface at higher temperatures should essentially be too hot to retain atomic Na, the surface chemistry must be sufficiently rapid to convert and so bind it. The chemical rates must be faster than the normal collisional kinetic rebound.

Above 800 K, as will be outlined in more detail in later publications, the data begin to fall away and become more scattered. This will not be discussed further here other than to indicate that for carbonate this in fact reflects the onset of what might be termed chemical vaporization, wherein the Na_2CO_3(s) ablatively vaporizes and is in a dynamic kinetic balance with gaseous NaOH and CO_2.

Deposits Formed at Lower Probe Temperatures and on the Burner Top

At the beginning of this program emphasis was placed on collecting deposits on probes above 600 K and invariably the deposit was pure Na_2CO_3. As mentioned already, after burning a flame for several hours it is quite normal for a deposit also to form as a honeycomb shape on top of the inner core of the multiholed flat flame burner. Such deposits are more pronounced

with slower burning (lower flow rate) propane flames and are much reduced for the faster flow rates associated with hydrogen fueled flames. It has been standard to analyze such burner top samples along with those collected on the probe in the flame. The burner is heated to about 50°C by recirculating warm water to minimize aerosol deposition within its core. Initially, in all cases, Na_2CO_3 deposits appeared to be dominant on the burner top but there also were apparent indications of some of the nebulized aerosol salt. In most of the earlier work $NaNO_3$ solutions were used as the aerosol sodium source so it appeared reasonable that some of it might collect on top of the burner as it was carried into the flame. However, two things were particularly noteworthy in these initial experiments. Firstly, in all the studies that involved addition of sulfur to the flame [1], either as a gas (SO_2) along with the $NaNO_3$ solution aerosol, or solely as Na_2SO_3 or $Na_2S_2O_3$ solution aerosols, the only component ever collected on the burner top was Na_2SO_4. In such cases, the identity of the aerosol was always absent. Secondly, even though the burner top is relatively cool, there was never a hint in the sulfur free experiments of $NaHCO_3$ formation in any of the first hundred or so experiments.

Thermodynamic data for the carbonates of sodium and potassium now are quite accurately known and values for ΔH_f and S^0 are in close agreement [32–35]. That for $NaHCO_3$ also appears to be consistent [34–36] although the heat of formation in one tabulation [33] appears to be in serious error. The situation is least certain for $KHCO_3$ but even so ΔH_f appears to have been established to within $\pm$ 4 kJ mol^{-1} [33, 35, 37]. The others are all known to better than $\pm$ 2 kJ mole^{-1}. Also, sodium and potassium bicarbonates can be purchased, are stable at room temperature, and can be made by bubbling CO_2 through carbonate solutions. Gases can be purified from CO_2 by bubbling through hot solutions of K_2CO_3 [38]. More recently, Hayashi et al. [39] have suggested in fact a CO_2 mitigation method whereby K_2CO_3 can be utilized to remove the CO_2 from combustion flue gases. This invokes the reaction

$$K_2CO_3(s)+CO_2(g)+H_2O(g) = 2KHCO_3(s)$$

$$\Delta H_{298\ K} = -144 \pm 4\ \text{kJ mol}^{-1} \quad (1)$$

They indicate that this conversion of carbonate to bicarbonate is very efficient up to 150°C for potassium and although less efficient for sodium ($\Delta H_{298\ K} = -134 \pm 2$ kJ mol^{-1} for the corresponding reaction [1]) is similarly effective at temperatures below about 90°C. Tests with potassium carbonate at 100°C using simulated flue gases containing 13.4% CO_2 and 11% H_2O validated its effectiveness. Fossil fueled flames, including the propane flames in this work, produce burned gases that are generally of the order of 10% CO_2 and 15% H_2O content. For such a mix, thermodynamic calculations similarly indicate that $NaHCO_3$ should be favored at temperatures below about 350 K, and for $KHCO_3$ below about 400 K. In hydrogen/air flames that contain about 100 ppm CO_2, these temperature limits lower to about 310 and 345 K, respectively. These data are all consistent with the well known fact that $NaHCO_3$ powder should not be stored in air at temperatures above 50°C or it decomposes [40]. Consequently, although somewhat marginal, we were surprised never to have observed $NaHCO_3$ formation. Additionally, measured activation energies for the reverse of reaction [1] with sodium, namely dissociation of $NaHCO_3$ are in the 100 to 130 kJ mol^{-1} range [41–43] implying that an energy barrier in reaction [1] should not be a kinetic limitation.

To examine this lack of bicarbonate deposition further, samples were collected in the flame with a water cooled probe at temperatures in the 332 to 373 K range, and with a greater variation of nebulized alkali salt solutions. Resulting deposit compositions are indicated for sodium in Fig. 10 and for potassium in Fig. 12 for fuel lean and rich propane flames. Initially the results were unexpected and as seen with sodium (Figs. 10 and 11), although Na_2CO_3 formation remains dominant, $NaNO_3$ begins to play a role, particularly under fuel lean conditions. In Fig. 10a, sodium glycinate $CH_2(NH_2)COONa$ solution is used as a source of both flame sodium and fuel nitrogen. Measured relative Raman cross sections for sodium carbonate and nitrate imply a 13% contribution of $NaNO_3$ to the deposit in Fig. 10a and about 5% in Fig. 10b when sodium oxalate is used in

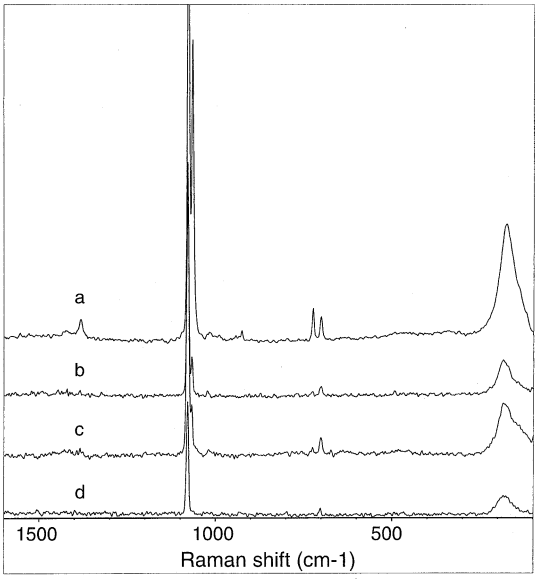

Fig. 10. Raman spectra of sodium deposits collected on a platinum clad probe cooled to low temperatures: (a) 332 K in a ϕ = 0.9 ($C_3H_8/O_2/N_2$, 0.9/5/16) flame, 5.3 ms downstream, sodium glycinate, $CH_2(NH_2)COONa$, nebulized aerosol, (b) 345 K, ϕ = 0.9 (C_3H_8/air) flame, 6.2 ms downstream, sodium oxalate nebulized aerosol, (c) 373 K, ϕ = 1.1 (C_3H_8/air) flame, 3.1 ms downstream, $NaNO_3$ nebulized aerosol, (d) 355 K, ϕ = 1.2 (C_3H_8/air) flame, 4.0 ms downstream, sodium oxalate nebulized aerosol.

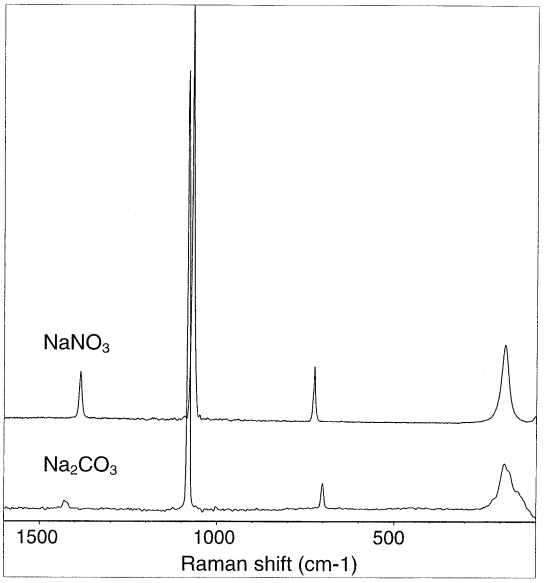

Fig. 11. Raman reference spectra of pure samples of Na_2CO_3 and $NaNO_3$ salts.

the nebulizer. On the fuel rich side there is only a slight indication of $NaNO_3$ being about 4% in Fig. 10c with $NaNO_3$ in the nebulizer. This appears very marginal as a corresponding run but with $NaNO_2$ indicated no formation of $NaNO_3$ on the probe. As seen in Fig. 10d, aspirating sodium oxalate produced only Na_2CO_3. In all these cases, the probe is at least about 3 to 4 ms (lean) or 5 to 6 ms (rich) downstream from the reaction zone and the nebulized salt is known to be fully dissociated as it leaves the reaction zone. As a result, there is no doubt that the nitrate observed on the probe is produced in competition and in preference to carbonate. $NaNO_3$ is thermally stable to about 653 K. As to whether enhanced levels of flame NO_x increase the role of $NaNO_3$ has yet to be examined but would seem to be a reasonable expectation.

The flame data for potassium are indicated in Fig. 12 with spectra of pure compounds shown in Fig. 13. It is even more intriguing and quite unexpected. Under lean conditions the nitrate again is clearly evident and more significant. It is thermally stable to about 673 K. Figs. 12a and 12b both represent mixtures of about 68% K_2CO_3 and 32% KNO_3. In this case the data are the same whether KNO_2 or potassium formate (HCOOK) is in the nebulizer. Under rich conditions, however, as seen in Figs. 12c and 12d the deposit changes its nature completely. The Raman spectrum of potassium oxalate, $(COOK)_2$, becomes clearly evident and in Fig. 12c, for the first time, there is an indication of some $KHCO_3$ formation. Correcting the intensities for the relative scattering cross sections, Fig. 12c implies a deposited mixture of 42% K_2CO_3, and 29% each of the oxalate and bicarbonate. The distribution in Fig. 12d shows a more pronounced formation of the oxalate and the composition is about 84% oxalate and 16% carbonate. As seen clearly in Fig. 13, the Raman spectrum of potassium oxalate is very characteristic and easily identifiable. It is thermally stable to about 743 K, whereas sodium oxalate, not evident in any of these experiments, is thermally stable to about 523 K. It is obvious at these low temperatures that although the rate of deposition still remains the same, as to what the alkali forms is in a more delicate balance, controlled by flame equivalence ratio and other flame parameters which need to be examined further.

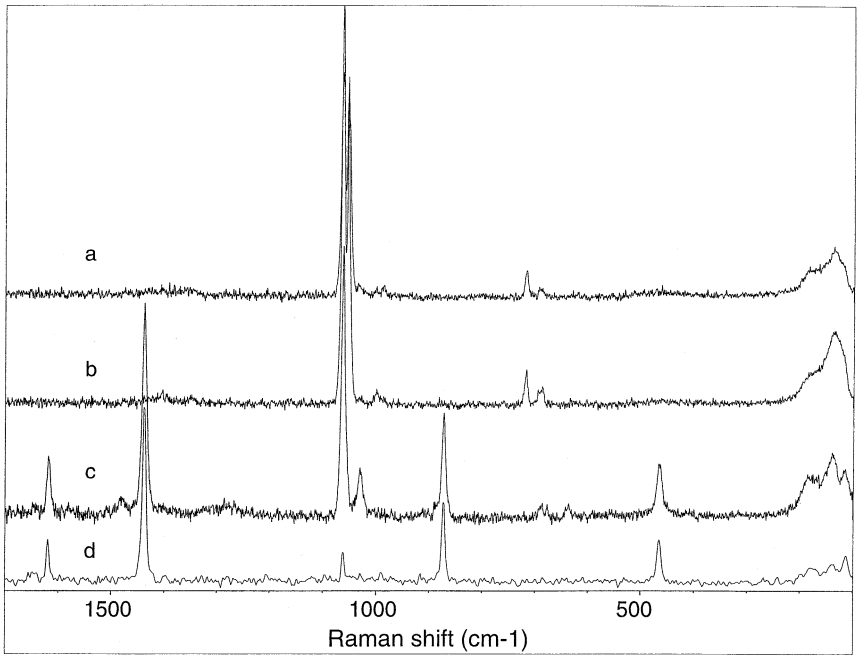

Fig. 12. Raman spectra of potassium deposits collected on a platinum clad probe cooled to low temperatures: (a) 332 K, KNO_2 nebulized aerosol, (b) 335 K, potassium formate nebulized aerosol, both in $\phi = 0.9$ ($C_3H_8/O_2/N_2$, 0.9/5/16) flames, 5.3 ms downstream, (c) 335 K, potassium formate nebulized aerosol, (d) 332 K, KNO_3 nebulized aerosol, both in $\phi = 1.1$ ($C_3H_8/O_2/N_2$, 1.1/5/20) flames, 5.8 ms downstream.

It has been very fortunate that the FT Raman spectral analysis method is so ideally suited to analyze these more involved alkali salt mixtures.

On reflection, the concept of thermodynamic equilibrium on the probe surface tends to hold little meaning in the present situation. It is an open system with the flame impinging on the surface. From the surface's point of view the flame is far from equilibrium. In a system at 330 K and at equilibrium, atoms and radicals do not exist. Table 1 examines the relative thermodynamic stabilities of the carbonates, bicarbonates, nitrates, and oxalates for sodium and potassium. Near room temperature, indications are that the thermodynamic preferential ordering is nitrate>bicarbonate>carbonate>oxalate. Consequently, the observation of nitrate on the probe and burner top is not unreasonable but it appears to be controlled by flame parameters (and possibly availability of NO_x) on the fuel lean side, and is largely suppressed under rich conditions. Bicarbonate formation is certainly expected over that of the carbonate but is largely not seen. Recently, Plane et al. [46] have noted that in the gas-phase, reaction of $NaHCO_3$(g) with H-atom is effective even at low temperatures. It is possible that a similar reaction is occurring on the probe and burner top surfaces, the H-atom preventing $NaHCO_3$(s) formation. However, a small amount of $KHCO_3$(s) was noted in a fuel rich-flame, questioning to some degree the rationality of such an argument.

These observations raise the question as to whether oxides of nitrogen in realistic flue gases will interfere with the CO_2 flue gas mitigation method based on K_2CO_3 /$KHCO_3$ conversion as recently proposed by Hayashi et al. [39].

The most intriguing observation of potassium oxalate formation under fuel rich conditions on the flame probe (but not the burner top) indicates that there are interesting kinetic aspects. The flame species are undoubtedly perturbing the surface chemistry and overriding thermodynamic considerations. Nevertheless, the constancy of deposition rate indicates that the alkali still is retained by the surface despite everything and the kinetic balances modify to satisfy a preferred distribution of products.

The formation of potassium oxalate was to-

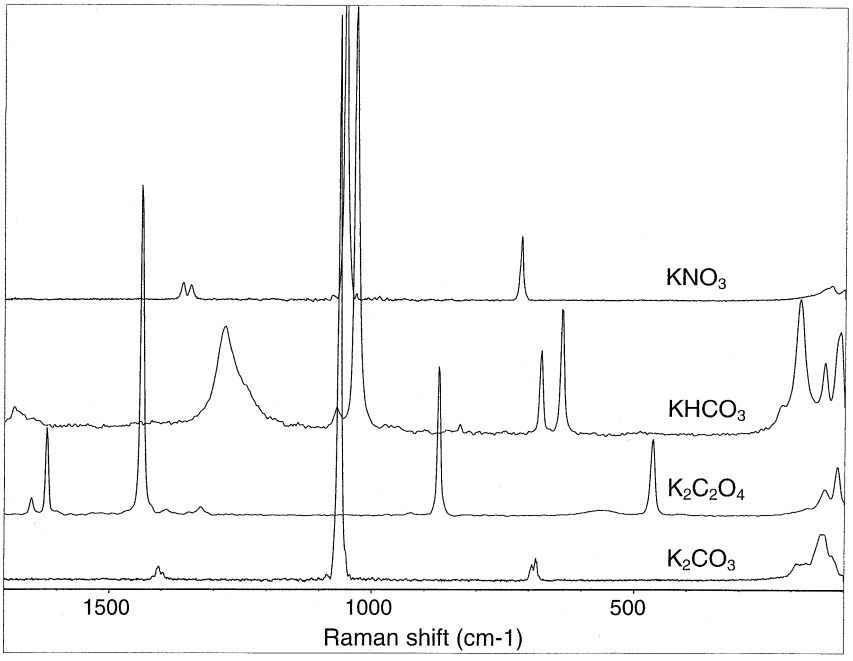

Fig. 13. Raman reference spectra of pure samples of KNO_3, $KHCO_3$, potassium oxalate, $(COOK)_2$, and K_2CO_3 salts.

tally unexpected. It is our first observation of clearly non-equilibrium deposit formation from flames. The natural implication might be that room temperature cooled surfaces immersed in flames may hold promise as a technique for the synthesis of non-equilibrated or metastable molecular structures. We plan a more detailed study of potassium oxalate formation on 300 to 500 K probes in a variety of rich flames including $H_2/O_2/N_2$ in which the flame carbon can be controlled. Oxalate $(COOK)_{2,}$ is in essence a double carbonate, the K:C ratio being 1:1 instead of the normal 2:1 of K_2CO_3, and is thermally stable to about 743 K.

Similar non-equilibrium behavior has never been observed by us in systems containing sulfur. As already mentioned, Na_2SO_4 always appears to be dominant, presumably because of its very pronounced thermodynamic stability. We have monitored no other sulfur-bearing compound even with low collection probe temperatures. Although not studied very extensively, the

TABLE 1

Relative Thermodynamic Stabilities of Solid Carbonates, Bicarbonates, Oxalates, and Nitrates of Sodium and Potassium at 300 K[a]

	M=Na		M=K	
	ΔH(kJ mol^{-1})	K_p(atm)	ΔH(kJ mol^{-1})	K_p(atm)
$M_2CO_3+CO_2+H_2O(g) = 2MHCO_3$	−135	7.5 (5)[b]	−143	6.9 (7)
$M_2C_2O_4+H_2O(g)+0.5O_2 = 2MHCO_3$	−336	—	−341	—
$M_2C_2O_4+0.5O_2 = M_2CO_3+CO_2$	−201	—	−198	—
$M_2CO_3+2NO_2+0.5O_2 = 2MNO_3+CO_2$	−265	5.0 (31)	−298	2.3 (38)
$2\ MHCO_3+2NO_2+0.5O_2 = 2MNO_3+2CO_2+H_2O(g)$	−129	6.7 (25)	−154	3.3 (30)
$M_2C_2O_4+2NO_2+O_2 = 2MNO_3+2CO_2$	−466	—	−495	—

[a] Based on thermochemical values for Na_2CO_3, CO_2, H_2O, NO_2, O_2 [32], K_2CO_3, $KHCO_3$ [33], $NaHCO_3$ $NaNO_3$, KNO_3 [36] and $Na_2C_2O_4$, $K_2C_2O_4$ [44, 45].

[b] Read 7.5(5) as 7.5×10^5.

same is expected to apply to K_2SO_4 which is significantly more stable than Na_2SO_4 [47].

Burner Top Deposition Mechanism

With the present flat flame burner there is a narrow stand-off distance of about 0.5 mm between the burner top and the flat reaction zone that is stabilized by a certain heat loss to the burner. As outlined already, a water cooled probe in the flame can be adjusted to have approximately the same temperature as the burner top (about 325 K) and the deposits on the two compared. Figure 14 gives a representation of the nature of several burner top samples for a variety of flame equivalence ratios and nebulized salts. Figure 14a corresponds to the flame probe data of Fig. 10a. Unlike the probe that displays sodium carbonate and nitrate, only carbonate is observed on the burner top. A solution of $CH_2(NH_2)COONa$ was the aerosol source. Figure 14b, for a lean H_2 flame also shows solely carbonate and no signs of the $NaNO_3$ aerosol. Figure 14c, a fuel rich-flame with $\phi = 1.2$ propane/air and a sodium oxalate aerosol also indicates a pure carbonate deposit on both the burner top and on a flame probe at a similar temperature (Fig. 10d). Figure 14d, a similar run but with $\phi = 1.1$, indicates both nitrate and carbonate on the burner top using an $NaNO_2$ solution aerosol. Figure 14e that corresponds with Fig. 12c shows potassium carbonate, nitrate and bicarbonate on the burner top, but oxalate, carbonate and bicarbonate on the flame probe.

The alkali on the burner top can presumably result from both back diffusion from the reaction zone and from aerosol condensation followed by conversion. In all cases of Fig. 14 the deposits do not reflect the aerosol in any way and any such direct aerosol deposit, if occurring, is modified by the differing reactive chemical environments. The situation on the burner top differs from the probe's impinging flame environment and this is apparently reflected in the observed variations. The absence of $NaNO_3$ in Fig. 14a may result from a lack of NO_x in the reaction zone, but is similarly lacking in Fig. 14b when $NaNO_3$ is the aerosol, both under fuel lean conditions. More than anything, the formation of potassium oxalate on the probe (Fig. 12c) yet not on the burner top (Fig. 14e), where KNO_3 is favored, illustrates our present lack of understanding of the controlling mechanisms at these lower temperatures. The probe appears to favor nitrate formation under fuel lean conditions yet the burner top under fuel rich. The probe favoring potassium oxalate formation yet the burner top KNO_3 when the nebulizer salt solution is potassium formate and NO_x must be quite small in the flame's reaction zone. Some $KHCO_3$ appears on both the probe and burner top with HCOOK addition yet is absent on the probe for KNO_3 addition. Such disparate observations are the first results to be noted in this work that indicate a pivotal role for the flame rather than the surface.

Deposition Reversibility

In the temperature range 340 to 800 K deposition occurs irreversibly. Deposition rates are insensitive to flame non-equilibrium and radical ablation is negligible. If a deposit is produced on a flame probe and then the flame sodium addition cut off, a slight flame coloration can be seen above the probe indicating that some loss of sodium is occurring but at a negligible rate in this temperature range. The eye is extremely sensitive to resonance line emission of sodium. Deposition loss was quantified by producing a deposit and leaving it in a sodium free flame for a period of time. Up to 800 K a measurable loss could not be detected. However, 850 K appeared to be the threshold probe temperature for the onset of ablative loss of Na_2CO_3 and at 870 K in one measured case became about a 4% loss rate per hour, gradually accelerating as temperatures increased. This is reflected to some degree in the higher temperature data of Fig. 9 and illustrates the onset of a sensitivity of the rate to flame temperature and also to flame equilibration. A subsequent paper concerning the fall-off of deposition rates because of ablative evaporative loss will outline this different behavior at these more elevated probe temperatures.

Interconvertability of Carbonate Deposits

In a series of experiments, flames were burned containing traces of sodium, with and without sulfur additions. If a flame is burned containing

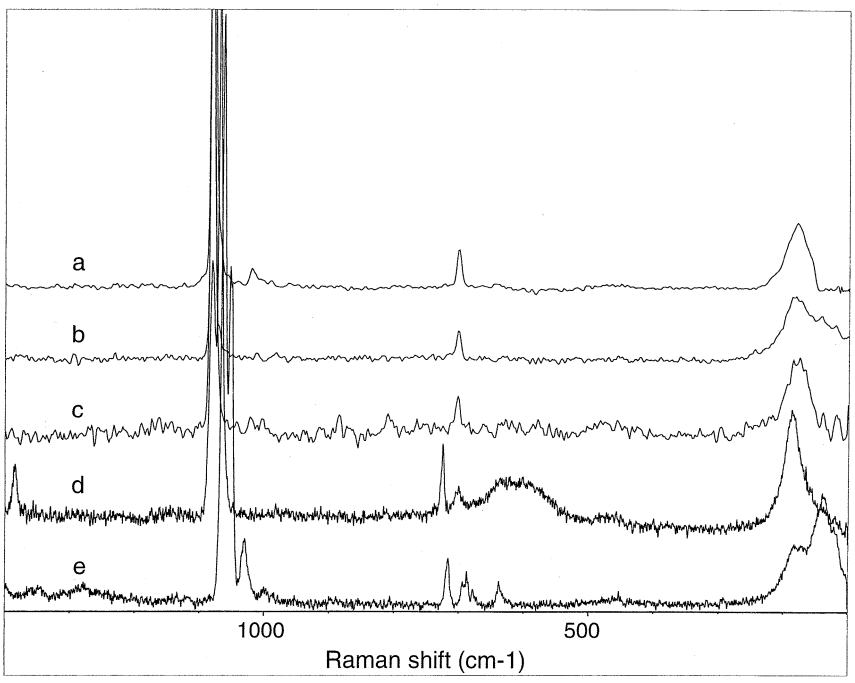

Fig. 14. Raman spectra of deposits collected as a honeycomb matrix build-up on top of the burner around the burner core holes. The burner was warmed by circulating water to about 325 K: (a) $\phi = 0.9$ ($C_3H_8/O_2/N_2$, 0.9/5/16) flame, sodium glycinate $CH_2(NH_2)COONa$ solution aerosol (corresponds with Fig. 10a probe data), (b) $\phi = 0.5$ ($H_2/O_2/N_2$, 1/1/3) flame, $NaNO_3$ solution aerosol, (c) $\phi = 1.2$ (C_3H_8/air) flame, sodium oxalate solution aerosol (corresponds with Fig. 10d probe data), (d) $\phi = 1.1$ ($C_3H_8/O_2/N_2$, 1.1/5/20) flame, $NaNO_2$ solution aerosol, (e) $\phi = 1.1$ ($C_3H_8/O_2/N_2$, 1.1/5/20) flame, HCOOK solution aerosol (corresponds to Fig. 12c probe data). All indicate carbonate formation, (d) and (e) nitrate, and (e) some bicarbonate.

sodium and sulfur, a deposit of Na_2SO_4 forms on a probe. If the sulfur addition then is turned off, the deposit continues to grow but is now Na_2CO_3 layering down on top of the initial sulfate. When removed, the Raman spectra shows these two components as in Fig. 15a and for equal times is a 50/50% mix. The peak at 994 cm^{-1} is due to Na_2SO_4 and that at 1080 cm^{-1}, Na_2CO_3. However, if the experiment is done in reverse, first laying down a carbonate deposit and then adding sulfur to the flame, not only is there a continued growth of a sulfate layer, but the flame sulfur converts the previous carbonate sub-layer also to sulfate. With sufficient sulfur, which implies sufficient for the formulation Na_2SO_4, the total deposit becomes Na_2SO_4. This is indicated in Figs. 15b and 15c for lean and rich equivalence ratios. In other words, flame sulfur converts carbonate deposits irreversibly to sulfate. On the molecular level, the flame sulfur, presumably SO_2, permeates into the Na_2CO_3 deposit, and modifies the crystal structure to that of Na_2SO_4 with the CO_2 being exhausted.

The other small peaks seen in Fig. 15 are extremely interesting. As already illustrated in Fig. 11, the Raman spectrum of Na_2CO_3 is quite simple and other than the strong line at 1080 cm^{-1} has only a weak line at 702 cm^{-1} in this spectral range above 400 cm^{-1}. Slight hydration of the carbonate can shift the major frequency to 1070 cm^{-1} for the hydrated salt. These three features are apparent in Fig. 15a, the carbonate having managed to pick up a little moisture during handling. All the other spectral features are due to Na_2SO_4. These, however, appear to be somewhat different in Fig. 15a, 15b, and 15c and in fact reflect different low temperature phases of Na_2SO_4. The Na_2SO_4 spectrum of Fig. 15a is noisy, but is typical of purchased Na_2SO_4(V) the stable phase at 0 to 458 K. Figure 15c is a clean spectrum of Na_2SO_4(III), a metastable structure obtained by cooling from temperatures above 517 K in the absence of

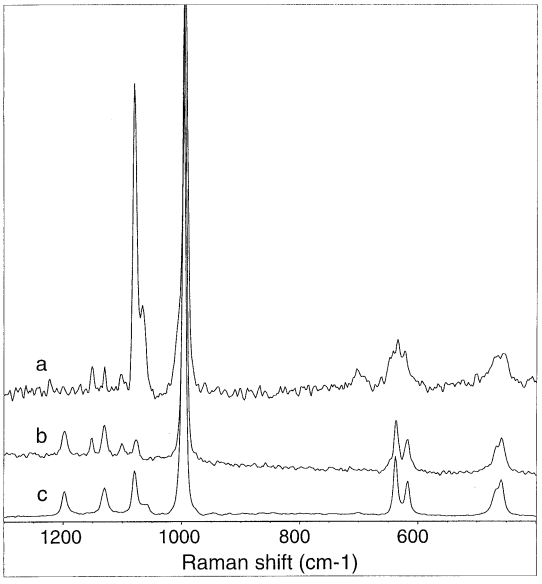

Fig. 15. Raman spectra of deposits collected on stainless steel probes at 725 K: (a) $\phi = 0.9$ (C_3H_8/air) initially with 45 ppm sodium and 500 ppm SO_2 flame content. Then continued without sulfur for the same length of time. Probe 6 ms downstream, (b) $\phi = 0.9$ (C_3H_8/air) burned similarly but initially with 45 ppm flame sodium only and then for the same length of time also with 500 ppm SO_2 added, (c) $\phi = 1.1$ (C_3H_8/air) burned initially with 30 ppm flame sodium only and then continued for the same length of time with 50 ppm SO_2 also added. Probe 5 ms downstream. The major peaks at 994 and 1081 cm^{-1} are those of Na_2SO_4 and Na_2CO_3, respectively.

moisture. Figure 15b indicates the presence of both (V) and (III) phases in the analyzed sample, indicating a partial structural relaxation. These alternate crystal structures, both orthorhombic, have different space group descriptions and produce this variation of fine structure frequency patterns [32, 48].

As will be outlined in subsequent papers in this series, similar conversions to that of Na_2CO_3 to Na_2SO_4 also are seen in Na/Cl systems when Na_2CO_3 also is readily converted irreversibly by chlorine to NaCl. The resulting conclusion is that sodium has a very pronounced preference for its anion. In the 400 to 900 K surface temperature regime this correlates with thermodynamic stabilities and demonstrates the ordering Na_2SO_4>NaCl>Na_2CO_3>NaOH. However, as seen for the first time in this paper, this very orderly behavior finally breaks down at temperatures below about 400 K.

CONCLUSIONS

The most noteworthy aspect of this work is the observation that Na_2CO_3 flame deposition behavior mirrors almost exactly that of Na_2SO_4. In the 400 to 800 K probe temperature range there are no differences. In fact, rates of deposition measured as the quantity of sodium alkali metal are identical, indicating the controlling aspect of the inflow of alkali and not its subsequent chemical formulation. Consequently, rates are seen to be first order in flame sodium concentration, zero order in flame carbon concentration and show the similar independence of flame or probe parameters, and even flame non-equilibrium conditions. Rates of deposition also are non-variant in the 330 to 800 K region, establishing a zero activation energy. The flame nature of the sodium, but it atomic, or the hydroxide also is irrelevant and either appear to have approximately similar surface accommodation coefficients and be converted equally to carbonate. This similar behavior of sulfate and carbonate deposition irrefutably establishes its heterogeneous nature. At low probe temperatures, <400 K, differences in the carbonate system do begin to emerge with respect to the chemical nature of the deposit but not its rate of deposition. Presumably, this arises from the reduced thermodynamic stabilities of Na_2CO_3 and K_2CO_3 and the opportunities for other molecules such as their nitrates, and in the case of potassium the oxalate and bicarbonate, to compete to be the anion of choice for the alkali. Whereas at higher temperatures the systems appears to be largely controlled by the thermodynamic stabilities, at low probe temperatures we see for the first time non-equilibrium behavior. The expectation of observing bicarbonate formation is not realized in the case of sodium, where instead contributions of $NaNO_3$ are apparent. This behavior is more pronounced in the case of potassium where under fuel lean conditions the deposit can approach a 70/30% mixture of K_2CO_3 and KNO_3, respectively, and under fuel rich conditions an unexpected significant presence of potassium oxalate, $K_2C_2O_4$, with carbonate and finally the observation of a fractional bicarbonate contribution. Toward room temperature, thermodynamic equilibrium preferences suggest the ordering nitrate>

bicarbonate>carbonate>oxalate. This observation of oxalate formation is extremely intriguing and shows the possibility that low temperature surfaces in flames may be a synthetic technique for the formation of thermodynamically metastable materials. The apparent role for the flame under these conditions indicates that the flame radicals are perturbing the expected thermodynamic chemical balances on the surface.

The collection efficiencies of alkali metals on flame probes have been further confirmed to be significantly large. Rates have also been studied in several C_3H_8/O_2 flames where the diluent was either He, Ne or Ar. These deposition rates remain unexplainable with current boundary layer-fluid dynamic models which at present appear to be an inadequate description.

Although not specifically related to high temperature corrosion, this study of Na_2CO_3 deposition has in fact added extensively to that very topic. It is a very good example in illustrating that research should not be micromanaged or too restricted. Valuable information can come from unexpected systems that are only loosely connected to what may be considered the major thrust.

The authors gratefully acknowledge the support of this work by the Chemical and Transport Systems Section of the National Science Foundation, Grant Number NSF CTS-9020355, monitored by Dr. M.J. Linevsky, and by the Electric Power Research Institute, Grant Number EPRI RP8005-15, monitored by Dr. A. Mehta. We sincerely appreciate their patience in permitting us to delay publication of this work until we had fully resolved the data to our satisfaction.

This work made use of the Material Research Laboratories Central Facilities which are supported by the National Science Foundation under Award No. DMR00-80034.

REFERENCES

1. Steinberg, M., and Schofield, K., *Proc. Combust. Inst.* 26:1835 (1996).
2. Stringer, J., *High Temp. Technol.* 3:119 (1985).
3. Gupta, A. K., Immarigeon, J.-P., and Patnaik, P. C., *High Temp. Technol.* 7:173 (1989).
4. Bryers, R. W., *Prog. Energy Combust. Sci.* 22:29 (1996).
5. Deadmore, D. L., Lowell, C. E., and Kohl, F. J., *Corrosion Sci.* 19:371 (1979).
6. Fryburg, G. C., Miller, R. A., Stearns, C. A., and Kohl, F. J., in *High Temperature Metal Halide Chemistry* (D. L. Hildenbrand and D. D. Cubicciotti, Eds.). The Electrochemical Society, Symp. Series 78–1, Princeton, NJ, 1978, p. 468.
7. Rosner, D. E., Chen, B.-K., Fryburg, G. C., and Kohl, F. J., *Combust. Sci. Technol.* 20:87(1979).
8. Stearns, C. A., Kohl, F. J., and Rosner, D. E., in *High Temperature Corrosion* (R. A. Rapp, Ed.). National Association of Corrosion Engineers, NACE-6, Houston, TX, 1983, p. 441.
9. Santoro, G. J., Gokoglu, S. A., Kohl, F. J., Stearns, C. A., and Rosner, D. A., in *High Temperature Corrosion in Energy Systems* (M. F. Rothman, Ed.). Metallurgical Society of AIME, New York, 1985, p. 417.
10. Gokoglu, S. A., and Santoro, G. J., in *High Temperature Alloys for Gas Turbines and Other Applications* (W. Betz, et al., Eds.). Conference Proceedings, Reidel Publishers, Dordrecht, The Netherlands, 1986, Part II, 1986, p. 1117.
11. Gokoglu, S. A., *J. Electrochem. Soc.* 135:1562 (1988).
12. Michelsen, H. P., Frandsen, F., Dam-Johansen, K., and Larsen, O. H., *Fuel Process. Technol.* 54:95 (1998).
13. Nielsen, H. P., Baxter, L. L., Sclippab, G., Morey, C., Frandsen, F. J., and Dam-Johansen, K., *Fuel* 79:131 (2000).
14. Kaufmann, H., Nussbaumer, T., Baxter, L., and Yang, N., *Fuel* 79:141 (2000).
15. Hansen, L. A., Nielsen, H. P., Frandsen, F. J., Dam-Johansen, K., Horlyck, S., and Karlsson, A., *Fuel Process. Technol.* 64:189 (2000).
16. Andersen, K. H., Frandsen, F. J., Hansen, P. F. B., Wieck-Hansen, K., Rasmussen, I., Overgaard, P., and Dam-Johansen, K., *Energy Fuels* 14:765 (2000).
17. Anthony, E. J., *Prog. Energy Combust. Sci.* 21:239 (1995).
18. Anthony, E. J., Talbot, R. E., Jia, L., and Granatstein, D. L., *Energy Fuels* 14:1021 (2000).
19. Newby, R. A., and Bannister, R. L., *J. Eng. Gas Turbines Power, Trans. ASME* 120:450 (1998).
20. Steinberg, M., and Schofield, K., *Prog. Energy Combust. Sci.* 16:311 (1990).
21. Schofield, K., and Steinberg, M., *J. Phys. Chem.* 96:715 (1992).
22. Dunderdale, J., and Durie, R. A., *J. Inst. Fuel* 37:493 (1964).
23. Dahiya, R. P., and Sharma, S. C., *J. Phys. D: Appl. Phys.* 27:263 (1994).
24. Hildenbrand, D. L., and Lau, K. H., *J. Phys. Chem*. 95:8972 (1991).
25. Ager, J. W., III, and Howard, C. J., *J. Geophys. Res.* 92:6675 (1987).
26. Rajasekhar, B., and Plane, J. M. C., *Geophys. Res. Lett.* 20;21(1993).
27. McNeil, W. J., Murad, E., and Lai, S. T., *J. Geophys. Res.* 100:16847 (1995).
28. Plane, J. M. C., Gardner, C. S., Yu, J., She, C. Y., Garcia, R. R., and Pumphrey, H. C., *J. Geophys. Res.* 104:3773 (1999).
29. Hynes, A. J., Steinberg, M., and Schofield, K., *J. Chem. Phys.* 80:2585 (1984).

30. Red'ko, T. P., *Sov. Phys. Tech. Phys.* 28:1065 (1983).
31. Dmitriev, S. P., and Dovator, N. A., *Tech. Phys., Russia* 39:343 (1994).
32. Chase, M. W., Jr., Davies, C. A., Downey, J. R., Jr., Frurip, D. J., McDonald, R. A., and Syverud, A. N., JANAF Thermochemical Tables, 3rd edition, *J. Phys. Chem. Ref. Data,* Volume 14, Supplement No. 1, 1985.
33. Knacke, O., Kubaschewski, O., and Hesselmann, K., Eds., *Thermochemical Properties of Inorganic Substances,* 2nd edition. Springer-Verlag, Berlin, 1991.
34. Kubaschewski, O., Alcock, C. B., and Spencer, P. J., *Materials Thermochemistry,* 6th edition. Pergamon Press, New York, 1993.
35. Wagman, D. D., Evans, W. H., Parker, V. B., Schumm, R. H., Halow, I., Bailey, S. M., Churney, K. L., and Nuttall, R. L., *The NBS Tables of Chem. Thermodynamic Properties: Selected Values for Inorganic C_1 and C_2 Organic Substances in SI Units, J. Phys. Chem. Ref. Data*, Volume11, Supplement No. 2, 1982.
36. Barin, I., and Platzki, G., *Thermochemical Data of Pure Substances,* 3rd edition. VCH Publishers, Weinheim, Germany, 1995.
37. Naumov, G. B., Ryzhenko, B. N., and Khodakovsky, I. L., *Handbook of Thermodynamic Data* Atomizdat, Moscow, 1971, U. S. Geological Survey Engl. Transl., January 1974, NTIS Report PB-226722.
38. Lyudkovskaya, M. A., Fridman, S. D., and Klevke, V. A., *Khim. Prom*. 41(5);339 (1965), (Russ), CA 63:3923g (1965).
39. Hayashi, H., Taniuchi, J., Furuyashiki, N., Sugiyama, S., Hirano, S., Shigemoto, N., and Nonaka, T., *Ind. Eng. Chem. Res.* 37:185 (1998).
40. Trees, D., and Seshadri, K., *Combust. Sci. Technol.* 122:215 (1997).
41. Ball, M. C., Snelling, C. M., Strachan, A. N., and Strachan, R. M., *J. Chem. Soc., Faraday Trans. I* 82:3709 (1986).
42. Tanaka, H., and Takemoto, H., *J. Thermal Analysis* 38:429 (1992).
43. Guarini, G. G. T., Dei, L., and Sarti, G., *J. Thermal Analysis* 44:31 (1995).
44. Brown, M. A. H., *The Heats of Formation of Selected Cyanide and Oxalate Compounds, Dissertation Abstracts: Sci. Eng.* 29B:3696 (1969), University Microfilms, Ann Arbor MI, Number 69–6530.
45. Brown, M. H., and Taylor, A. R., Jr., *U.S. Clearinghouse Fed. Sci. Tech. Inform*., PB Report No.04, 17 pp., 1970, CA 75:336 (1971).
46. Cox, R. M., Self, D. E., and Plane, J. M. C., *J. Geophys. Res.* 106:1733 (2001).
47. Stern, K. H., and Weise, E. L. *High Temperature Properties and Decomposition of Inorganic Salts. Part I. Sulfates,* National Standards Reference Data Series—National Bureau of Standards, NSRDS-NBS 7, 38 pp. (1966).
48. Hapanowicz, R. P., and Condrate, R. A., Sr., *Spectrosc. Lett*. 29:133 (1996).

Received 4 September 2001; revised 26 February 2002; accepted 13 March 2002